PLANAR ANTENNAS FOR PASSIVE UHF RFID TAG

A. Kumar and D. Parkash

Department of Electronics and Communication Engineering
Haryana College of Technology and Management
Ambala Road, Kaithal 136027, India

M. V. Kartikeyan

Department of Electronics and Computer Engineering
IIT Roorkee
Roorkee 247667, India

Abstract—In this paper, design, fabrication, and testing of Radio Frequency Identification (RFID) antennas for the European Telecommunications Standards Institute (ETSI) and Federal Communications Commission (FCC) bands are discussed. The designs proposed in this paper are for UHF RFID tag that conforms to EPCglobal C1G2 1.2.0. The exceptional characteristics of the RFID are investigated in terms of antenna-IC matching and radiation efficiency. The proposed RFID antennas have been fabricated on 5 mil thick Flexible Copper Clad Laminate and the read range of the proposed RFID antennas is experimentally tested. Measured free air read range of all proposed designs is over 4 m. The performance of the tag antenna design affixed to various objects is also tested with read range measurements. The results show that the antenna designs can be used for tagging cardboard and plastic objects.

1. INTRODUCTION

RFID applications are rapidly growing due to drop in both reader and tag prices and expansion of global markets. RFID tags are either powered by the reader (passive tags) or contain on-board power sources (semi-active and active tags). Some estimates indicate that as the price for the passive tag continues to fall, virtually every product sold will have a RFID tag in it. Traditional RFID systems working in the high

---

Corresponding author: A. Kumar (arun_ktl@rediffmail.com).

frequency (HF) and low frequency (LF) bands have limited range due to their near-field communication constraint. Backscattering RFID systems in the ultra high frequency (UHF) band, on the other hand, having the capability to achieve longer range, greater data rate and faster read speed, have rapidly attracted end users attention in the applications of supply chain, transportation, etc. [1].

Major hardware components of a RFID system are reader/interrogator, reader antenna and a RFID tag/transponder. Passive RFID tags do not have any internal source of energy. The IC is powered by the electromagnetic waves radiated by the reader that also communicates with the tag in order to get its data [2]. Communication in passive UHF RFID systems is based on backscattering of modulated electromagnetic wave: Reader transmits energy and commands to tag which then responds by backscattering its identification data back to reader using for example amplitude shift keying (ASK) modulation [3].

Because in passive RFID tag microchip is attached directly to an antenna, proper impedance match between the antenna and the chip is crucial in RFID tag design [4, 6–10]. It directly influences RFID system performance characteristics such as the range of a tag. Since new IC design and manufacturing is a big and costly venture, RFID tag antennas are designed for an application specific Integrated circuit (ASIC) available in the market. Adding an external matching network with lumped elements is usually prohibitive in RFID tags due to cost and fabrication issues. To overcome this situation, antenna can be directly matched to the ASIC which has complex impedance varying with the frequency and the input power applied to the chip [4, 9]. Effect of frequency on microchip input impedance values at various sensitivity levels is presented in more detail in [9]. To maximize the read range the antenna should be conjugate matched to the minimum operational power chip impedance [9].

RF tag performance is affected by many factors, including the electromagnetic properties of objects near or attached to the tag antenna. Often a tuneable antenna design is preferable to provide tolerance for tag fabrication variations and for optimizing antenna performance on different materials in different frequency bands [4]. In this paper, we explore structures of planar tag antennas with good impedance matching and tuneabilty. The designs presented in this paper are optimized using EM simulation tool for good free air read range. Antennas are designed for ETSI frequency band (865.7 MHz to 867.6 MHz) and FCC frequency band (902.75 MHz to 927.25 MHz) of UHF RFID. We performed the parametric study of proposed antenna designs so that tuning parameters of designs can be identified. Once the tuning parameters are known, antenna designs can be tuned for

attaching it on various materials. We have used flexible copper clad laminate for the designs proposed in this paper because its mechanical properties make it very much suitable for mechanically robust and reusable tags for the applications in which RFID tag is to be directly attached on object without plastic housing. The antennas are designed and analyzed with the aid of IE3D software, which is based on method of moments (MOM). The finalized designs are built on a 5 mil thick Flexible Copper Clad Laminate. Antenna designs are manufactured through a subtractive process where flexible copper clad laminates are chemically etched to remove all copper except that forming the antenna pattern. The prototypes of proposed designs are also tested practically using a UHF reader to check their free air read range and effect of various materials on their performance. Antennas were designed and implemented for NXP UCode Gen2 tag chip with impedance $22 - j404\,\Omega$ at $867\,$MHz and $16 - j380\,\Omega$ at $915\,$MHz measured at minimum operating power. Minimum operating power of NXP Ucode Gen2 tag chip at $867\,$MHz and $915\,$MHz is $-14\,$dBm and $-13\,$dBm respectively.

2. ANTENNA STRUCTURE

Compared to PET, flexible copper clad laminates have high tensile strength, low dielectric loss, solderability, subtractive process applicability making it suitable for easy and inexpensive fabrication of RFID antenna. From the cost point of view flexible copper clad laminate is expensive that PET, but mechanical properties of flexile copper clad make it suitable for reusable tags which compensate its higher cost. Antenna pattern on flexible copper clad laminate can be made using inexpensive screen printing and chemical etching. By Screen printing a resist on the copper clad was created to protect the antenna pattern in etching. TSSOP8 Chip bonding on flexible copper clad laminate based antenna can be done easily by normal soldering technique.

The structure of proposed Antenna 1 is shown in Figure 1. Antenna 1 consists of meandered line feed section, two rectangular sections and two loading bars. Two rectangular sections are incorporated in the design to increase the antenna impedance value. Impedance of Antenna 1 is mainly determined by the two rectangular sections. Two chip pads of size $1.5\,$mm $\times$ $2\,$mm are included in the design for easy attachment of TSSOP8 packaged microchip. In the proposed design a meandered feed line section is used because meandering allow the antenna to be compact and to provide omnidirectional performance in the plane perpendicular to the axis

of the meander [4, 5, 8]. To have a better control over the antenna impedance, two loading bar of width 1 mm are incorporated in the proposed design. The two loading bars are inductively coupled to feed line section and a separation of 1 mm between loading bars and meandered feed line section is included. Loading bars in the design help in Antenna impedance adjustment which is very important for impedance matching. Depending upon the chip impedance loading bars and rectangular sections length can be adjusted to achieve the impedance matching. Dimensions of the optimized antenna are shown in Figure 1. Physical size of Antenna 1 is 85 mm × 16.3 mm.

The structure of Antenna 2 is shown in Figure 2. The loading bar is inductively coupled to radiating section and a separation of 0.5 mm is kept between loading bars and radiating section. Loading bar in the proposed design is included for the fine adjustment of the antenna impedance ($Ra + jXa \, \Omega$). The impedance of antenna is mainly determined by the parameters W, Fl, L_1, and L_2. The geometric parameters are adjusted carefully and final optimized Antenna 2 dimensions are: $L = 59.5$ mm, $W = 43$ mm, $L_1 = 22.2$ mm, $L_2 = 4.39$ mm, $Fl = 38.85$, $Fw = 0.5$ mm, $Fg = 6.33$ mm, $Lb_1 = 62.5$ mm, $Lb_2 = 4.25$ mm. Physical size of Antenna 2 is 62.5 mm × 44.5 mm.

Figure 3 shows the structure of Antenna 3. The two inductively coupled loading bars 'A' and 'B' in the proposed design are included for the fine adjustment of the Antenna impedance ($Ra + jXa \, \Omega$). Meandered feed line section is used to reduce the antenna size [5, 8]. The impedance is mainly determined by the geometry parameters L, W and meandered feed line section. Antenna 3 optimized dimensions are: $L = 42.3$ mm, $W = 18.75$ mm, $Lb = 25.75$ mm, $Wa = 1$ mm, $Wb = 2$ mm, $W_1 = 2.25$ mm, $G_1 = 0.9$ mm, $G_2 = 0.85$ mm. Meandered
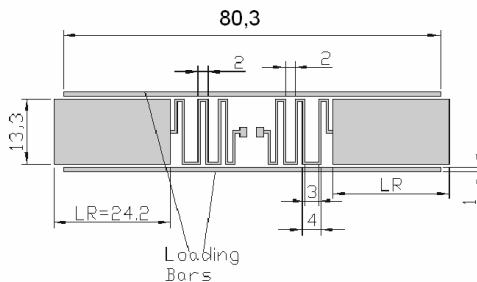

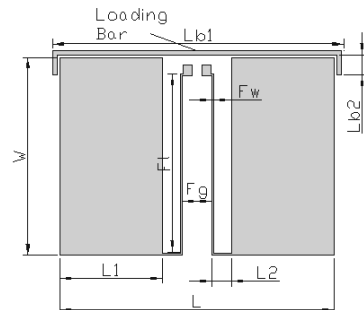**Figure 1.** Structure of proposed UHF RFID tag antenna 1.

Figure 2. Structure of proposed UHF RFID tag antenna 2.
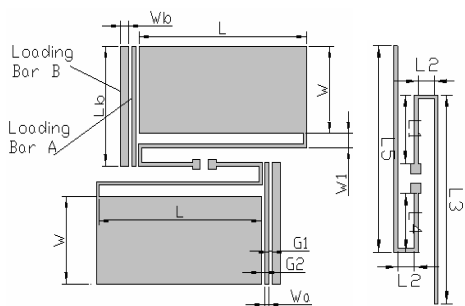
Figure 3. Structure and feed line section of proposed UHF RFID tag antenna 3.
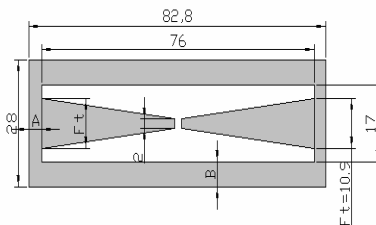

Figure 4. Structure of proposed UHF RFID tag antenna 4.

feed line section dimensions are: $FL_1 = L_1 + L_2 + L_3 = 58.85$ mm and $FL_2 = L_2 + L_4 + L_5 = 58.85$, where $L_1 = L_4 = 13.8$ mm, $L_2 = 3.25$ mm $L_3 = L_5 = 41.8$ mm. Physical size of Antenna 3 is 53.5 mm $\times 51.0$ mm.

Proposed Antenna 4 structure is shown in Figure 4. Antenna 4 is designed for FCC RFID frequency band. In the proposed design overall length of the structure determines the resonant frequency of the antenna. The tapered trace in the structures provides the capacitive impedance which can be made inductive by either increasing the taper or the length of taper trace. But it is observed that if we try to obtain inductive impedance by increasing taper angle and length of taper trace than antenna structure will be large with a very high value of real part of antenna impedance. So a rectangular ring with parameters 'A' and 'B' is included to obtain the inductive impedance without affecting much the real part of antenna impedance. Inductive rectangular ring also help in keeping antenna size compact. The main three parameters of Antenna 4 are 'A', 'B' and the feed line taper. Depending up on the chip impedance, parameters 'A' and 'B' and feed line taper are adjusted properly to obtain the desired input impedance. Optimized value of parameter 'A' and 'B' are: $A = 3.65$ mm, $B = 5.5$ mm. Other optimized dimensions of antenna 4 are shown in Figure 4. Physical size of Antenna 4 is 82.8 mm $\times 28$ mm.

3. RESULTS STUDY

Zealand's IE3D MOM based simulation tool is used for the simulation results study of the proposed designs. Antenna 1, Antenna 2 and Antenna 3 are designed for ETSI RFID frequency band while Antenna 4 is designed for FCC RFID frequency band. As the

proposed antennas Antenna1, Antenna 2 and Antenna 3 are designed for NXP Gen2 UCode IC, so proposed antennas parameters are adjusted for impedance close to $22 + j404\,\Omega$ at 867 MHz. Figure 5 shows the simulated results of real and imaginary values of Antenna 1 impedance $(Ra + jXa\,\Omega)$. Loading bars, rectangular section length and the meandered feed line section are adjusted for getting the desired impedance value. From the simulated results it can be seen that Antenna 1 impedance $(Ra + jXa\,\Omega)$ at 867 MHz frequency is $22.2 + j396\,\Omega$. Figure 6 shows the simulated radiation efficiency of the proposed design. It can be seen from figure that Antenna 1 efficiency at 867 MHz is 36.5%. Simulated directivity of Antenna 1 is 2.07 dBi at 867 MHz. The effect of two rectangular sections length and loading bars is also studied. Table 1 shows the Impedance values for different values of rectangular sections length keeping other parameters constant. In the study of rectangular sections effect no loading bars are included in the design. From the results shown in Table 1 it can be seen that antenna impedance is mainly determined by the two rectangular sections. Table 2 shows the antenna impedance values for different length of loading bars. From the result presented in Table 2 it can be seen that with the increase in the loading bars length real value of antenna impedance decreases while imaginary value of antenna impedance increases. In other words we can say that lading bars provide inductive effect and helps in fine adjustment of antenna impedance. We also compared the simulated gain of

Table 1. Antenna 1 rectangular section length (LR) effect.

LR (mm)	No Rectangular section	10.2 mm	14.2 mm	16.2 mm	20.2 mm	24.2 mm
Ra $+jXa\,(\Omega)$	4.9 $-j342\,\Omega$	16.12 $-j24.77\,\Omega$	21.28 $+j49.7\,\Omega$	24.22 $+j84.33\,\Omega$	30.97 $+j149\,\Omega$	39.06 $+j211\,\Omega$

No loading bar, other dimensions kept as shown in Figure 1.

Table 2. Loading bar length effect.

loading bar length (mm)	Lower bar only (80.3 mm)	Upper bar only (80.3 mm)	No bars	74.3 mm	76.3 mm	80.3 mm
Ra $+jXa\,(\Omega)$	26.29 $+j314\,\Omega$	24.97 $+j338.8\,\Omega$	39.24 $+j213\,\Omega$	24.05 $+j366\,\Omega$	23.27 $+j384\,\Omega$	22.2 $+j396\,\Omega$

$LR = 24.2\,\text{mm}$, other dimensions kept as shown in Figure 1.
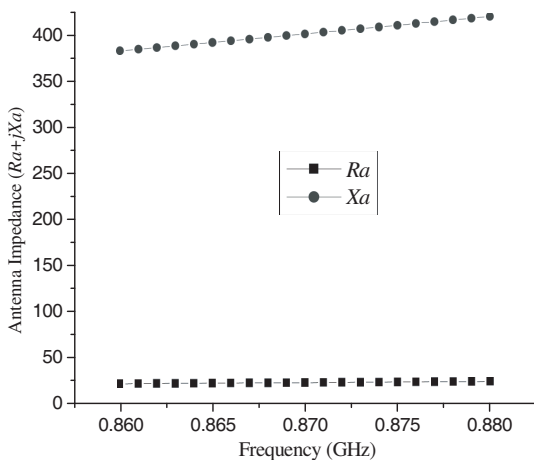
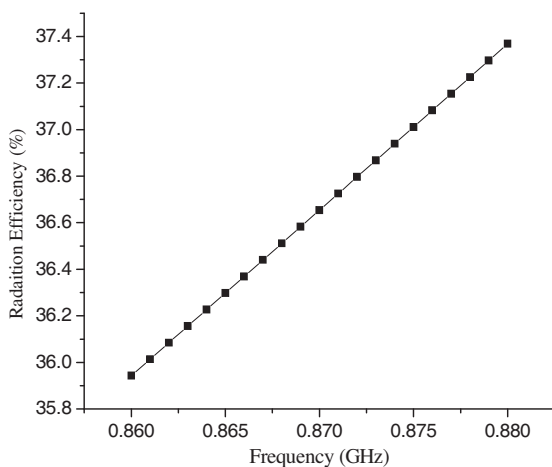**Figure 5.** Simulated results of antenna 1 impedance.

Figure 6. Simulated results of antenna 1 radiation efficiency.

Antenna 1 and a simple meander line dipole and observed that gain parameter of a simple meander line dipole is less than the Antenna 1 gain parameter. It shows that two rectangular sections in Antenna 1 helped in increasing the gain or effective area of the Antenna 1.

Figure 7 shows the simulated return loss of the optimized design when the antenna is conjugate-matched with the commercial tag chip (NXP Ucode). The simulated bandwidth is 2% ($S_{11} \leq -10$ dB) from 863 to 880 MHz, a 17 MHz bandwidth. ETSI frequency band for UHF RFID is from 865.7 MHz to 867 MHz.
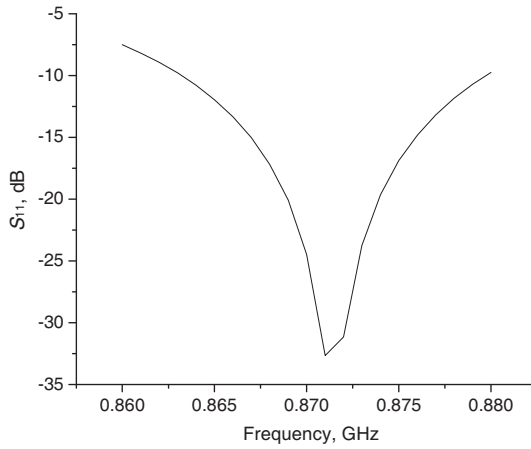
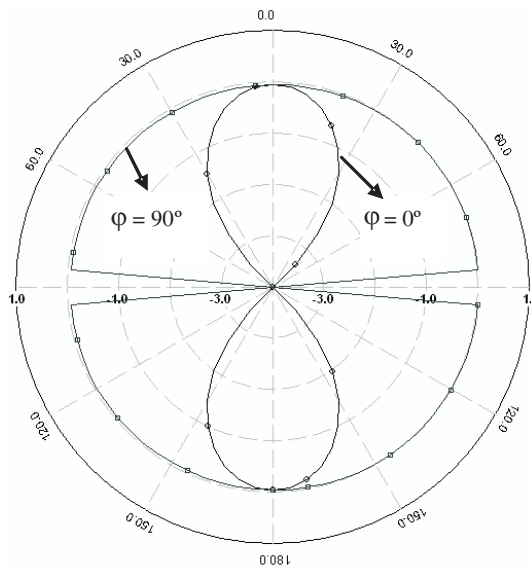**Figure 7.** Simulated return loss versus frequency plot of antenna 1.

Figure 8. Elevation pattern display of antenna 1.

In Figure 8, the 2-D radiation plots are shown. The 2-D polar plot shows the radiation in the two different planar cuts for the x-z plane ($\varphi = 0\,\mathrm{deg}$) and the y-z plane ($\varphi = 90\,\mathrm{deg}$) with angle θ that varies from 0 to 360 degrees. The pattern has two nulls in the whole 360

degree coverage area. This pattern similar to the radiation pattern of a half-wavelength dipole antenna as antenna 1 is also a dipole antenna.

Figure 9 shows the simulated results of real and imaginary values of Antenna 2 impedance ($Ra + jXa\,\Omega$). From the simulated impedance versus frequency graph it can be seen that Antenna 2 impedance ($Ra + jXa\,\Omega$) at 867 MHz frequency is $22.83 + j400.8\,\Omega$. From simulation results study it is observed that Loading bar length ($Lb = Lb_1 + Lb_2$) helps in fine adjustment of imaginary part (Xa) of the antenna impedance. Loading bar length has very small effect on real part of impedance (Ra). Xa values for different loading bar length keeping all other parameters constant are presented in Table 3. Effect of other parameter Fl, L_1 and W are presented in Tables 4–6. From the results shown in Tables 4–6 it is clear that antenna impedance is very much affected by Fl, L_1, and W. It can be seen from the results that geometry parameter W has slight effect on real part of

Table 3. Effect of loading bar length Lb on antenna impedance.

(Lb) mm	No bar	$Lb_1 = L$ mm $Lb_2 = 0$ mm	$Lb_1 = 62.5$ mm $Lb_2 = 0$ mm	$Lb_1 = 62.5$ mm $Lb_2 = 1.25$ mm	$Lb_1 = 62.5$ mm $Lb_2 = 3.25$ mm	$Lb_1 = 62.5$ mm $Lb_2 = 4.25$ mm
jXa (Ω)	j312.7 Ω	j382.5 Ω	j384.1 Ω	j387.2 Ω	j395.5 Ω	j400.8 Ω

$L = 59.5\,\text{mm}$, $W = 43\,\text{mm}$, $L_1 = 22.2\,\text{mm}$, $L_2 = 4.39\,\text{mm}$, $Fl = 38.85$, $Fw = 0.5\,\text{mm}$, $Fg = 6.33\,\text{mm}$.

Table 4. Effect of feed line length Fl on antenna impedance.

Fl (mm)	38.5 mm	36.5 mm	34.5 mm	32.5 mm	30.5 mm
Ra	22	20.56	18.66	17.02	15.63
$+jXa\,\Omega$	$+j400.8\,\Omega$	$+j367\,\Omega$	$+335.6\,\Omega$	$+j335.6\,\Omega$	$+j278.6\,\Omega$

$L = 59.5\,\text{mm}$, $W = 43\,\text{mm}$, $L_1 = 22.2\,\text{mm}$, $L_2 = 4.39\,\text{mm}$, $Fw = 0.5\,\text{mm}$, $Fg = 6.33\,\text{mm}$, $Lb = 63.13$, $Lb_1 = 5.25\,\text{mm}$.

Table 5. Effect of rectangular section length L_1 on antenna impedance.

L_1 (mm)	22.2 mm	21.2 mm	20.2 mm	19.2 mm	18.2 mm
Ra	22	21	19.96	19.55	18.59
$+jXa\,(\Omega)$	$+j400.8\,\Omega$	$+j380.4\,\Omega$	$+366.8\,\Omega$	$+j356.9\,\Omega$	$+j344.6\,\Omega$

$L = 59.5\,\text{mm}$, $W = 43\,\text{mm}$, $L_2 = 4.39\,\text{mm}$, $Fl = 38.85$, $Fw = 0.5\,\text{mm}$, $Fg = 6.33\,\text{mm}$, $Lb = 63.13$, $Lb_1 = 5.25\,\text{mm}$

Table 6. Effect of rectangular section width W on antenna impedance.

W (mm)	43 mm	42 mm	41 mm	40 mm	39 mm
Ra	22	21.71	21.3	20.99	20.65
$+jXa\,\Omega$	$+j400.8\,\Omega$	$+j352.6\,\Omega$	$+328.8\,\Omega$	$+j311.7\,\Omega$	$+j297\,\Omega$

$L = 59.5\,\text{mm}$, $L_1 = 22.2\,\text{mm}$, $L_2 = 4.39\,\text{mm}$, $Fl = 38.85$, $Fw = 0.5\,\text{mm}$, $Fg = 6.33\,\text{mm}$, $Lb = 63.13$, $Lb_1 = 5.25\,\text{mm}$.
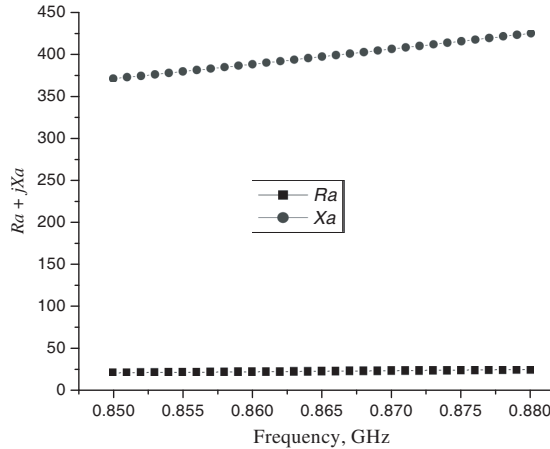

Figure 9. Simulated results of antenna 2 impedance.

antenna impedance while its effect on imaginary value is considerable. It can also be seen from the results that feed line length Fl effect on real part of antenna impedance is more than the other geometry parameters. Figure 10 shows the simulated radiation efficiency of the proposed design. It can be seen from figure that Antenna 2 efficiency at 867 MHz is 35%. Simulated directivity of antenna 2 is 1.92 dBi at 867 MHz.

Figure 11 shows the simulated return loss of the optimized design. The simulated results shows that antenna bandwidth ($S_{11} \leq -10\,\text{dB}$) is from 860 to 877 MHz, and capable to cover to ETSI frequency band for UHF RFID.

Radiation plots of antenna 2 in two different planar cuts for the x-z plane ($\varphi = 0\,\text{deg}$) and the y-z plane ($\varphi = 90\,\text{deg}$) are shown in Figure 12. The 2-D polar plot shows that the pattern has two nulls in the whole 360 degree coverage area. Antenna 2 pattern is similar to the radiation pattern of a half-wavelength dipole antenna because antenna 2 structure is like a bent dipole antenna.
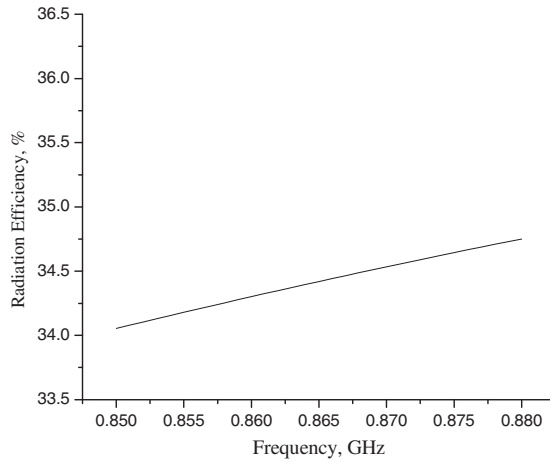
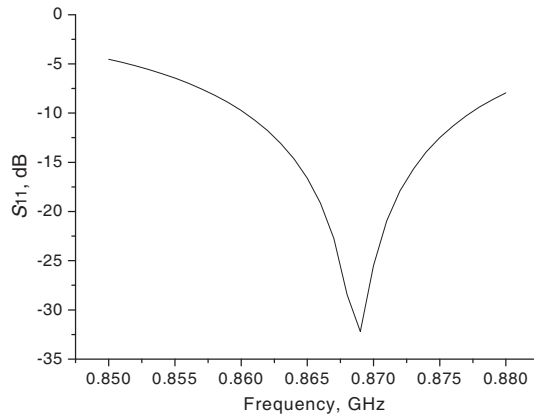**Figure 10.** Simulated results of antenna 2 radiation efficiency.

Figure 11. Simulated return loss versus frequency plot of antenna 2.

Table 7. Effect of rectangular section length L on antenna impedance.

L (mm)	37.3 mm	39.3 mm	40.3 mm	41.3 mm	42.3 mm
Ra	20.9	21.6	22.11	22.67	23.34
$+jXa\,(\Omega)$	$+j321.7\,\Omega$	$+j347\,\Omega$	$+j364.8\,\Omega$	$+j383.3\,\Omega$	$+j404\,\Omega$

$W = 18.75\,\text{mm}$, $Lb = 25.75\,\text{mm}$, $Wa = 1\,\text{mm}$, $Wb = 2\,\text{mm}$, $W_1 = 2.25\,\text{mm}$,
$G_1 = 0.9\,\text{mm}$, $G_2 = 0.85\,\text{mm}$, $FL_1 = 58.85\,\text{mm}$ and $FL_2 = 58.85$.

Simulated impedance of Antenna 3 is shown in Figure 13. Simulated impedance of proposed Antenna 3 design at 867 MHz is $23.34 + j404\,\Omega$. Effect of geometry parameter L and W are shown in Table 7 and Table 8. From the results it can be seen that effect of L and W on imaginary part of impedance is almost similar, but W variations have more effect on real part of impedance than the L variations. Feed line variation effect is shown in Table 9. Loading bars 'A' and 'B' helps in fine adjustment of the antenna impedance. Simulated radiation efficiency of Antenna 3 is 70% at 867 MHz (Figure 14). Simulated directivity of antenna 3 is 2.14 dBi at 867 MHz. Simulated return loss of the optimized design is shown in Figure 15. The simulated bandwidth is from 860 to 873 MHz ($S_{11} \leq -10\,\mathrm{dB}$), and completely covers the ETSI frequency band (865.7 MHz to 867 MHz) for UHF RFID.

In Figure 16, the 2-D radiation plots are shown. The 2-D polar plot shows the radiation in the two different planar cuts for the x-
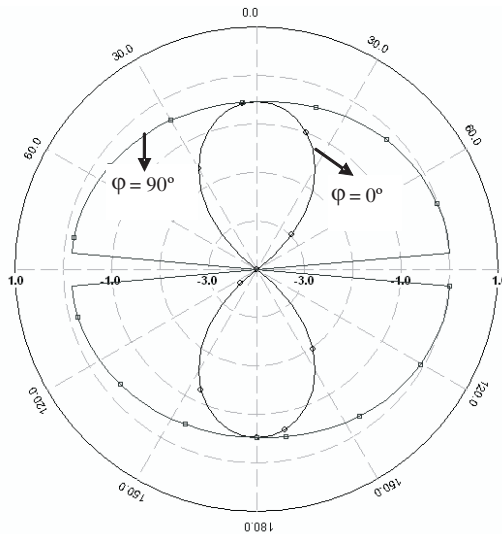

Figure 12. Elevation pattern display of antenna 2.

Table 8. Effect of rectangular section width W on antenna impedance.

W (mm)	14.75 mm	15.75 mm	16.75 mm	17.75 mm	18.75 mm
Ra	16.45	17.97	19.63	21.42	23.34
$+jXa\,(\Omega)$	$+j330.7\,\Omega$	$+j349\,\Omega$	$+j367.6\,\Omega$	$+j386\,\Omega$	$+j404\,\Omega$

$L = 42.3\,\mathrm{mm}$, $Lb = 25.75\,\mathrm{mm}$, $Wa = 1\,\mathrm{mm}$, $Wb = 2\,\mathrm{mm}$, $W_1 = 2.25\,\mathrm{mm}$, $G_1 = 0.9\,\mathrm{mm}$, $G_2 = 0.85\,\mathrm{mm}$, $FL_1 = 58.85\,\mathrm{mm}$ and $FL_2 = 58.85$.

z plane ($\varphi = 0\,\text{deg}$) and the y-z plane ($\varphi = 90\,\text{deg}$) with angle θ that varies from 0 to 360 degrees. The pattern is similar to the radiation pattern of a half-wavelength dipole antenna because antenna 3 structure is also like a bent dipole antenna.

Antenna 4 is designed for FCC RFID frequency band. NXP Gen2 Ucode IC provide impedance $16 - j380\,\Omega$ at $915\,\text{MHz}$, so Antenna 4 parameters 'A', 'B' and feed line taper are adjusted to get antenna impedance close to $16 + j380$. It is observed from the study of effect of parameter 'A' and 'B' (Table 10 and Table 11)
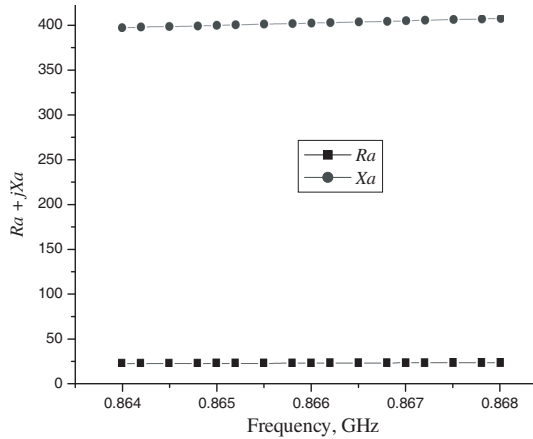
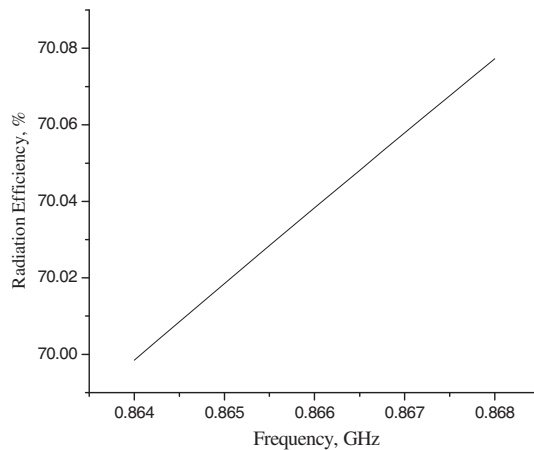**Figure 13.** Simulated results of antenna 3 impedance.

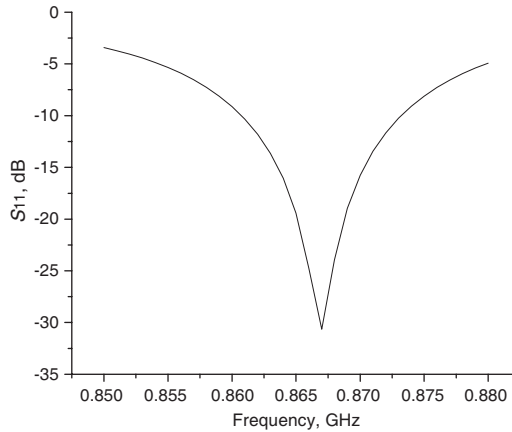**Figure 14.** Simulated results of antenna 3 radiation efficiency.

Figure 15. Simulated return loss versus frequency plot of antenna 3.

that if we increase the value of 'A' and 'B' antenna impedance value decreases. It is also observed that decrease in feed line taper increase the antenna impedance (Table 12). These variations show that by properly adjusting these parameters Antenna 4 impedance can be easily adjusted for other UHF EPC Gen2 ICs. Simulated impedance and efficiency results of the design are shown in Figure 17 and Figure 18 respectively. From Simulated impedance result of the Antenna 4 shown in Figure 17, it can be seen that impedance of the proposed design at 915 MHz is $15.9 + j380.2\,\Omega$. Simulated antenna efficiency is 60% at 915 MHz. Simulated directivity of Antenna 4 is 2.36 dBi at 915 MHz

Figure 19 shows the simulated return loss of the optimized design when the antenna is conjugate-matched with the commercial tag chip (NXP Ucode). The simulated bandwidth is 2.5% ($S_{11} \leq -10\,\text{dB}$) from 905 to 928 MHz. This encompasses almost the entire frequency range of FCC frequency band (902.75 MHz to 927.25 MHz) for UHF RFID.

The 2-D radiation plots in the two different planar cuts for the x-z plane ($\varphi = 0\,\text{deg}$) and the y-z plane ($\varphi = 90\,\text{deg}$) with angle θ that varies from 0 to 360 degrees are shown in Figure 20. The 2-D polar plot shows that the radiation pattern has two nulls in the whole 360 degree coverage area. The pattern is similar to the radiation pattern of a half-wavelength dipole antenna because antenna 4 structure is also a dipole with tapered arms.

Figures 21–24 show the direction of current flow in proposed designs. From the figures presented it can be seen that current direction in Antenna 1 and Antenna 2 are such that they add up destructively for the far field. From the current flow in antenna 1
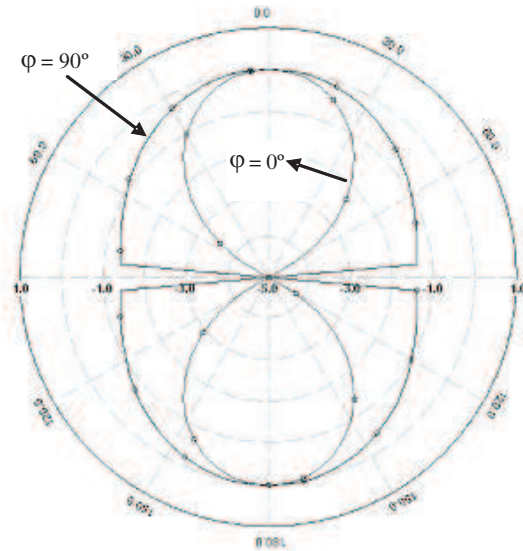
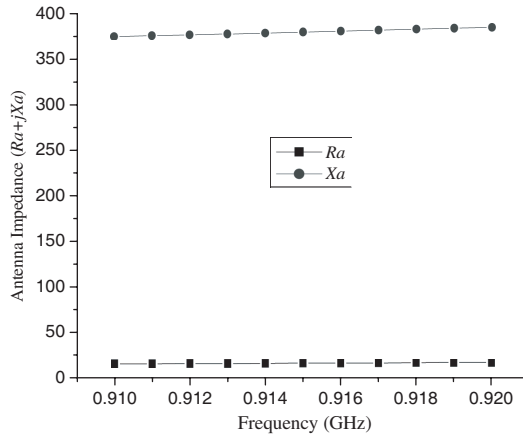**Figure 16.** Elevation pattern display of antenna 3.

Figure 17. Simulated results of antenna 4 impedance.

and antenna 2 it can be observed that if we increase the gap between meanders in antenna 1 and length L_2 (Figure 2) in Antenna 2 radiation efficiency can be increased, but it will also increase the physical size of the antenna. To verify this point we increased the length L_2 in Antenna 2 by 2 mm on both side without changing the fg value and checked the efficiency value. As the change in length L_2 also
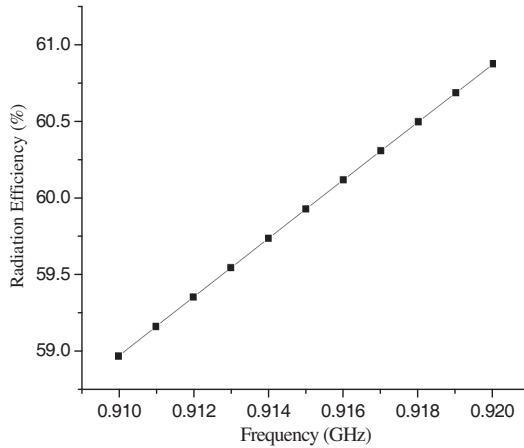
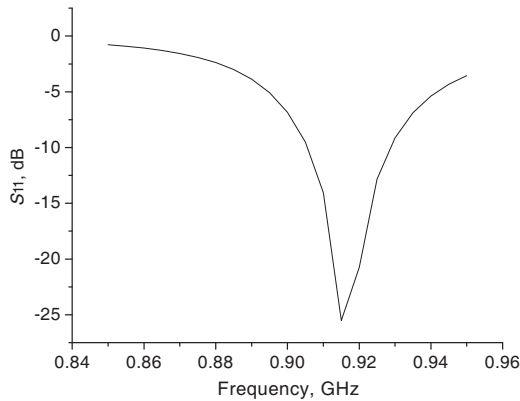**Figure 18.** Simulated results of antenna 4 radiation efficiency.

Figure 19. Simulated return loss versus frequency plot of antenna 4.

changes the impedance value so we adjusted Fl parameter to obtain the conjugate matching. We obtained a 39.6% simulated efficiency value which is 5% more than the previous value of simulated efficiency. Major factor for the high efficiency of antenna 3 and antenna 4 is because of the way the current flow. Since the direction of current flow in Antenna 3 and antenna 4 add up constructively for far-field radiation, the radiation efficiency of Antenna 3 and Antenna 4 is more than the antenna efficiency of Antenna 1 and Antenna 2.

A theoretical read range study of all proposed designs is also done on the basis of obtained simulated radiation efficiency and simulated
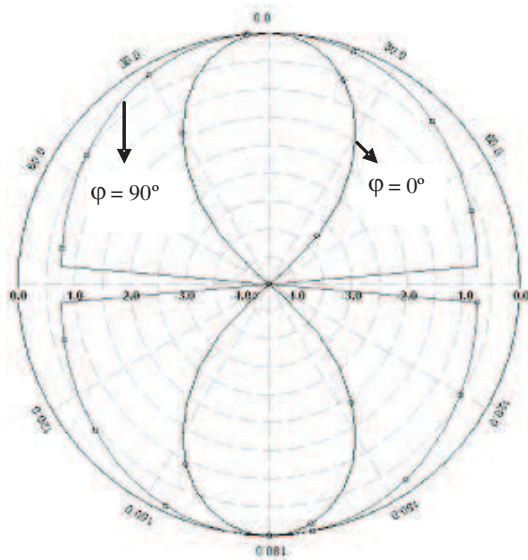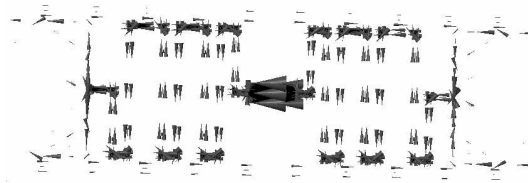
Figure 20. Elevation pattern display of antenna 4.

Figure 21. Simulated current flow in antenna 1.

Table 9. Effect of meandered feed line section length on antenna impedance.

FL_1 & FL_2 (mm)	$L_1=L_4$=9.8 mm $L_3=L_5$=37.8 mm	$L_1=L_4$=10.8 mm $L_3=L_5$=38.8 mm	$L_1=L_4$=11.8 mm $L_3=L_5$=39.8 mm	$L_1=L_4$=12.8 mm $L_3=L_5$=40.8 mm	$L_1=L_4$=13.8 mm $L_3=L_5$=41.8 mm
Ra+jXa (Ω)	$15.81+j286$ Ω	$17.07+j310$ Ω	$18.58+j335.3$ Ω	$20.48+j365.4$ Ω	$23.34+j404$ Ω

$L = 42.3\,\text{mm}$, $W = 18.75\,\text{mm}$, $Lb = 25.75\,\text{mm}$, $Wa = 1\,\text{mm}$, $Wb = 2\,\text{mm}$, $W_1 = 2.25\,\text{mm}$, $G_1 = 0.9\,\text{mm}$, $G_2 = 0.85\,\text{mm}$, $L_2 = 3.25\,\text{mm}$.
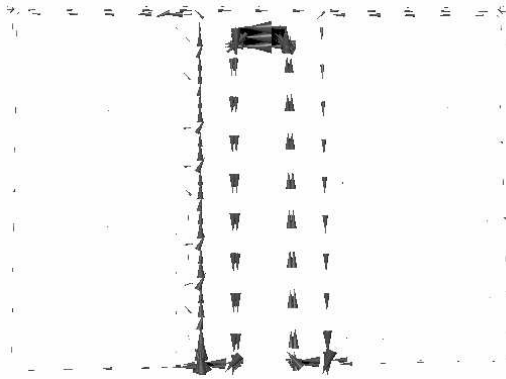
Figure 22. simulated current flow in antenna 2.
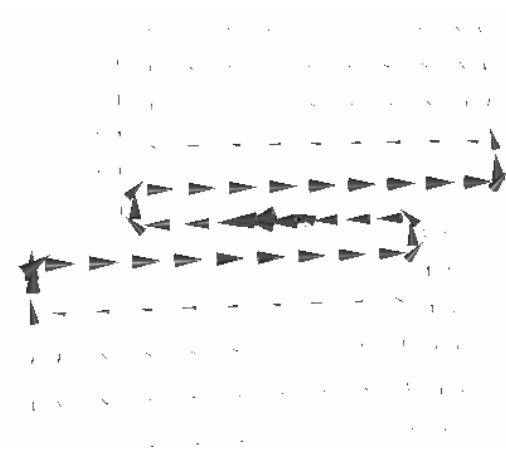

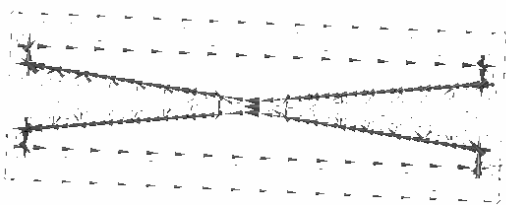**Figure 23.** simulated current flow in antenna 3.

Figure 24. simulated current flow in antenna 4.

directivity. The read range is calculated using the free space formula [4]

$$r = \frac{\lambda}{4\pi}\sqrt{\frac{P_t G_t G_r p\tau}{P_{th}}}$$

Table 10. Effect of parameter 'A'.

A (mm)	3.65 mm	4.65 mm	5.65 mm	7.65 mm	9.65 mm	11.65 mm
Ra	15.93	14.7	13.28	11.59	10.1	8.55
$+jXa\,(\Omega)$	$+j380.2\,\Omega$	$+j362.5\,\Omega$	$+j345.3\,\Omega$	$+j317.4\,\Omega$	$+j291\,\Omega$	$+j265.6\,\Omega$

Antenna length = 82.8 mm, Antenna width = 28 mm, $Ft = 10.9$ mm, $B = 5.5$ mm.

Table 11. Effect of parameter 'B'.

B (mm)	5.5 mm	6.5 mm	7.5 mm	4.5 mm	3.5 mm	3.9 mm
Ra	15.93	11.39	8.74	23.22	36.28	19.96
$+jXa\,(\Omega)$	$+j380.2\,\Omega$	$+j328.6\,\Omega$	$+j284.2\,\Omega$	$+j440\,\Omega$	$+j521\,\Omega$	$+j515\,\Omega$

Antenna length = 82.8 mm, Antenna width = 28 mm, $Ft = 10.9$ mm,
$A = 3.65$ mm.

Table 12. Effect of feed line taper.

Ft (mm)	10.9 mm	9.9 mm	8.9 mm	7.9 mm	5.9 mm	3.9 mm
Ra	15.93	16.19	16.84	17.35	18.46	19.96
$+jXa\,(\Omega)$	$+j380.2\,\Omega$	$+j393\,\Omega$	$+j410\,\Omega$	$+j427\,\Omega$	$+j465\,\Omega$	$+j515\,\Omega$

Antenna length = 82.8 mm, Antenna width = 28 mm, $A = 3.65$ mm,
$B = 5.5$ mm.

where λ is the wavelength, P_t is the power transmitted by the reader, G_t is the gain of the transmitting antenna, G_r is the gain of the receiving tag antenna, P_{th} is the minimum threshold and p is the polarization efficiency which should be 1/2 for most conventional case of circular-to-linear polarization mismatch. τ is the power transmission coefficient given by

$$\tau = \frac{4RcRa}{|Zc + Za|^2}, \quad 0 \leq \tau \leq 1$$

where $Zc = Rc + jXc$ is chip impedance and $Za = Ra + jXa$ is antenna impedance. Theoretically calculated results based on above formulas are shown in Table 13.

Table 13. Theoretically calculated read range.

	$P_t G_t$ (W)	Theoretically calculated Read range (m)
Antenna 1	3.3 W	4.32 m
Antenna 2	3.3 W	4.1 m
Antenna 3	3.3 W	5.9 m
Antenna 4	4 W	5.3 m

4. FABRICATION AND TEST RESULTS

The proposed antennas are fabricated by flexible copper clad laminate with $\varepsilon_r = 3.5$ and thickness 5 mil. Simple screen printing and chemical etching is used for fabrication. Prototypes of proposed antennas are shown in Figure 25 and Figure 26. Chip is attached to the antennas by manual soldering. Fabricated antennas performance is judged by testing their read range performance. Read range performance of the proposed antenna designs is measured with the help of Sirit IN510 fixed Reader and a single, circularly polarized antenna, of gain 6.5 dBi. Both reader and antenna can operate in 860 MHz to 960 MHz frequency band. The reader automatically calculates the conducted power level for reader antenna based on the regulatory region. The calculation takes into account antenna gain and cable loss settings. Conducted power level variation is required because as per the European Telecommunications Standards Institute (ETSI) and Federal Communications Commission (FCC) regulations maximum

Figure 25. Prototype of the proposed antenna 1 and antenna 2.

Figure 26. Prototype of the proposed antenna 3 and antenna 4.

allowed effective isotropic radiated power (EIRP) ratings are 3.3 W (or 2 W ERP) and 4 W respectively. For read range measurement of Antenna 1–Antenna 3 RFID reader is set to ETSI frequency band (865.7 MHz–867 MHz) and to FCC frequency band (902.75 MHz–927.25 MHz) for Antenna 4. Measurement set up was installed in an empty big hall. For free air read range measurement antennas were attached to very thin strings in a plastic frame. To find out the read distance the tag was first kept at very large distance from the reader and moved slowly towards the reader antenna. The distance at which reader detected the tag continuously was measured and recorded. We repeated the same procedure 5–6 times for each tag to verify the result.

RF tag performance is affected by many factors, including the electromagnetic properties of objects near or attached to the tag antenna. Since the resonance frequency of antenna changes when placed on a material, so many common materials have strong effects on the performance of UHF tag antenna. In worst case, tags may become unreadable ([11, 12]). To test the Effect of various materials on read range of the proposed designs we also measured the read range of the designs by attaching the antennas on plastic box, cardboard box and wooden box. We also tested the near metal performance of the proposed designs. The measured results are presented in Table 14. From the result presented in Table 14 it can be seen that free air read range of all designs proposed in this paper is good. Antenna 1 sensitivity is very high comparatively to other designs. If we compare the on plastic read range of Antenna 2–Antenna 4 designs it can be seen that plastic material have not much effect on proposed antennas resonance frequency and that is why antennas performance on plastic is comparable to their free air read range performance. In case of card board read range of Antenna 1–antenna 3 has reduced to 50%–60% than their read range in free space and on plastic box. It means card board have considerable effect on antennas impedance value. There is no effect of card board on read range of antenna 4. Antenna 1–antenna 3 performance on wood and near metal surface is very poor, which means wood and metal have very major effect on antennas resonance frequency. Antenna 4 performance on wood and near metal is acceptable. Less sensitivity of antenna 4 comparatively to other proposed designs may be because of the large FCC bandwidth of reader. For measurement of antenna 4 reader is set for frequency band 902.75 MHz–927.25 MHz. So even after the shift in resonance frequency of antenna 4, due to the materials effect, shifted resonant frequency of antenna 4 may lie with in the bandwidth range of reader. Large read range of antenna 4 comparatively to other proposed designs can also be due to the reason that allowable EIRP is more in FCC band than

the ETSI band. From the measured results it is clear that proposed designs provide acceptable read range for cardboard and plastic box and need tuning to get good read range for various materials in specific frequency band. Tuning of proposed designs for various materials is to be carried out in future work.

A comparison between theoretical (Table 13) and experimentally (Table 14) measured read range for all the proposed tags shows that theoretical data and experimental data are in close agreement. Measured values of Antenna 1, Antenna 2 and Antenna 4 are more than theoretically calculated value while Antenna 3 has shown an opposite behavior. Antenna 3 measured read range is less than the expected value which may be due to the shift in resonant frequency after the fabrication. As the simulated directivity of all proposed designs is approximately same, so it can be said that higher radiation efficiency can help in getting larger read range.

Table 14. Measured results of proposed antennas.

	Free Air	On Card Board	On wood	On Plastic	Near Metal (10 mm above from the metal surface)
Antenna 1	17.25 m	3 m	1 m	2 m	0.3 m
Antenna 2	5 m	3.5 m	1 m	5 m	0.45 m
Antenna 3	4.5 m	2.5 m	1 m	4.25 m	0.02 m
Antenna 4	7 m	7.5 m	5 m	8 m	3 m

5. CONCLUSION

Four passive RFID tag antenna Designs for ETSI and FCC UHF RFID frequency bands are proposed. All the designs are simulated to have good conjugate matching to commercially available NXP Gen2 UCode Chip. Low cost Flexible Copper Clad Laminate is used for prototypes fabrication. The prototypes of the designs are fabricated and tested for read range performance. Read range is measured by attaching the antennas on various objects for checking the material dependency on antennas performance. Measured results shows that the proposed antenna designs can be used for UHF RFID application. From the simulation studies it is clear that all the antennas have various tuning parameters which can be adjusted properly for optimizing antenna performance on different materials. From the measured results we can say that proposed designs with the dimensions mentioned in this paper are suitable for RFID tagging on cardboard and plastic boxes.

REFERENCES

1. Finkenzeller, K., *RFID Handbook: Fundamentals and Applications in Contactless Smart Cards and Identification*, John Wiley & Sons Ltd., West Sussex, Englnad, 2003.

2. Curty, J.-P., M. Declercq, C. Dehollain, and N. Joehl, *Design and Optimization of Passive RFID System*, Springer, New York, USA, 2007.

3. Ukkonen, L., M. Schaffrath, D. W. Engels, L. Sydänheimo, and M. Kivikoski, "Operability of folded microstrip patch-type tag antenna in the UHF RFID bands within 865–928 MHz," *IEEE Antennas and Wireless Propagation Letters*, Vol. 5, 414–417, 2006.

4. Rao, K. V. S., P. V. Nikitin, and S. F. Lam, "Antenna design for UHF RFID tags: A review and a practical application," *IEEE Transactions on Antennas and Propagation*, Vol. 53, No. 12, 3870–3876, 2005.

5. Kwon, H. and B. Lee, "Meander line RFID tag at UHF band evaluated with radar cross sections," *APMC Proceedings*, 2005.

6. Diugwu, C. A., J. C. Batchelor, R. J. Langley, and M. Fogg, "Planar antenna for passive radio frequency identification [RFID] tags," *IEEE Africon*, 2004.

7. Son, H. W. and C. S. Pyo, "Design of RFID tag antennas using an inductively coupled feed," *Electronics Letters*, Vol. 41, No. 18, 2005.

8. Gaetano, M., "The art of UHF RFID antenna design: Impedance — Matching and size reduction techniques," *IEEE Antennas and Propagation Magazine*, Vol. 50, No. 1, 66–79, 2008.

9. Loo, C. H., K. Elmahgoub, F. Yang, A. Elsherbeni, D. Kajfez, A. Kishk, and T. Elsherbeni, "Chip impedance matching for UHF RFID tag antenna design," *Progress In Electromagnetics Research*, PIER 81, 359–370, 2008.

10. Nikitin, P. V. and K. V. S. Rao, "Antennas and propagation in UHF RFID systems," *2008 IEEE International Conference on RFID The Venetian*, 277–288, Las Vegas, Nevada, USA, Apr. 16–17, 2008.

11. Dobkin, D. M. and S. M. Weigand, "Environmental effects on RFID tag antennas," *Proc. IEEE Int. Microw. Symp.*, Jun. 2005.

12. Griffin, J. D., G. D. Durgin, A. Haldi, and B. Kippelen, "RF tag antenna performance on various materials using radio link budgets," *IEEE Antennas and Wireless Propagation Letters*, Vol. 5, 2006.